Quantifying the effect of *A. thaliana* root on antibiotic production in the beneficial bacterium, *B. subtilis*

Harsh Maan[1], Omri Gilhar[1], Ziv Porat[2] and Ilana Kolodkin-Gal[1]

[1] Department of Molecular Genetics, Weizmann Institute of Science, Rehovot, Israel

[2]Flow Cytometry Unit, Life Sciences Core Facilities, Weizmann Institute of Science, Rehovot, Israel

Corresponding author: Ilana.kolodkin-gal@weizmann.ac.il

Abstract

Beneficial and probiotic bacteria play an important role in conferring the immunity of their hosts against a wide range of bacterial, viral and fungal diseases. *B. subtilis* is a bacterium that protects the plant from various pathogens due to its capacity to produce an extensive repertoire of antibiotics. At the same time, the plant microbiome is a highly competitive niche, with multiple microbial species competing for space and resources, a competition that can be determined by the antagonistic potential of each microbiome member. Therefore, regulating antibiotic production in the rhizosphere is of great significance to eliminate pathogens and to establish beneficial host-associated communities.

In this work, we used *Bacillus subtilis* as a model to investigate the role of plant colonization in antibiotic production. Flow cytometry and Image-stream cytometry analysis supported the notion that *A. thaliana* specifically induced the transcription of the biosynthetic clusters for the non-ribosomal peptides surfactin, bacilysin and plipastatin and the polyketide bacillaene. This induction could be beneficial for the root as all clusters were shown to antagonize plant pathogens. Consistently, the root failed to induce PenP, a β-lactamase that increases only the fitness of the bacteria. Our results can be translated to improve the performance and competitiveness of beneficial members of the plant microbiome.

Introduction

Rhizobacteria can promote plant growth directly by colonization of the root and exert beneficial effects on plant growth and development (Kloepper et al., 2004a). These bacteria are often designated plant growth-promoting rhizobacteria (PGPR). To date, various PGPR have been isolated, including various *Bacillus* species, *Burkholderia cepacia and Pseudomonas fluorescens.* These beneficial rhizobacteria can also confer fitness on their hosts by activating their immune system, and by antagonizing plant pathogens (Berg et al., 2017; Berg and Raaijmakers, 2018; Allaband et al., 2019). In addition to the direct promotion of plant growth, PGPR enhance the efficiency of fertilizers, and aid in degrading xenobiotic compounds (Adam et al., 2016; Berg et al., 2017).

Among growth promoting strains and biocontrol agens, *Bacillus subtilis* and its related species, such as *B. amyloliquefaciens, B. velezensis and B. mojavensis* are considered model organisms (Fan et al., 2017). In particular, the antimicrobial activity of *B. subtilis* was so far demonstrated against bacterial, viral and fungal soil-borne plant pathogens (Kloepper et al., 2004b; Nagorska et al., 2007). This activity is mediated largely by antibiotic production*:* approximately 5% of the *B. subtilis* genome is dedicated to the synthesis of antimicrobial molecules by non-ribosomal peptide synthetases (NRPS) or polyketide synthases (PKS/NRPS) (Stein, 2005; Ongena and Jacques, 2008; Kinsella et al., 2009). *In vitro* and *in planta* studies indicated the importance of four antibiotics for plant protection: surfactin, bacilysin, plipastatin and bacillaene (Hou and Kolodkin-Gal, 2020; Arnaouteli et al., 2021).

Surfactin, is a small cyclic lipopeptide induced during the development of genetic competence (Magnuson et al., 1994). The machinery for surfactin synthesis is encoded within the *srfAA–AB–AC–AD* operon (Kluge et al., 1988). Surfactin is a powerful surfactant with antibacterial (Gonzalez et al., 2011) and antifungal properties (Falardeau et al., 2013).

Bacilysin is a non-ribosomal dipeptide composed of L-alanine and amino acid L-anticapsin, that demonstrates antibacterial activity against a wide range of pathogens **(**Rajavel *et al.*, 2009). Its synthesis is controlled mainly by the *bac* operon (*bacABCDE)* and is regulated by other enzymes such as thymidylate synthase, homocysteine methyl transferase and the oligopeptide permeases (Inaoka et al., 2003).

Fengycin/plipastatin (Tsuge et al., 2007) is a highly effective lipopeptide comprising 10 amino synthetized by five fengycin synthetases (*ppsA, ppsB, ppsC, ppsD, and ppsE*).

61 Bacillaene and dihydrobacillaene (Butcher et al., 2007; Straight et al., 2007) are polyketides
62 synthesized by an enzymatic complex encoded in the *pks* gene cluster (Butcher et al., 2007;
63 Straight et al., 2007). This linear antimicrobial macrolides are synthesized by the PKSJLMNR
64 cluster mega-complex (Straight et al., 2007).

65 Interestingly, we recently found that the plant host can enhance the efficiency of the killing of
66 *Serratia plymuthica by B. subtilis* by inducing the synthesis of the antibiotic baceilaene (Ogran
67 et al., 2019). These preliminary results raise the question on whether additional antibiotics that
68 contribute to rhizocompatibility are induced by the plant to promote the colonization of preferred
69 symbionts. To address this question, we considered the overall effect of the plant host in
70 regulating four major antibiotics: surfactin, bacillaene, bacilysin and plipstatin, and an unrelated
71 antibiotic resistance gene, the beta-lactamase PenP.

72 Our results indicate that the attachment with the root can specifically enhance antibiotic
73 production (but not the β-lactamase PenP) and therefore affect the competitiveness of root-
74 associated bacteria compared with their free-living counterparts.

75

76 **Results**

77 Using flow cytometry, we examined the expression of transcriptional reporters P_{srfAA}-yfp, P_{pksC}-
78 mKate, P_{bacA}-gfp and P_{ppsA}-gfp in static cultures. Specifically, we asked whether association
79 with the plant would impact their expression. For this purpose, we compared bacteria cultured
80 in liquid medium with bacteria attached to plant roots. The number of cells expressing each
81 NRP and their respective mean intensity of fluorescence both increased for all these antibiotics'
82 promoters. In addition, the mean intensity of cells expressing from the *pps* and *pks* operons
83 also increased (Figure 1).

84 Conventional flow cytometry allows accurate high-throughput quantification of fluorescence
85 intensities, however it is less accurate for bacterial analysis. Higher fluorescence levels may be
86 interpreted as higher expression levels, but also can result from larger bacterial size or small
87 aggregates. Therefore, to increase our resolution into the manner by which antibiotic promoters
88 respond to the attachment of the root we used Imaging Flow Cytometer. By collecting large
89 numbers of digital images per sample and providing a numerical representation of image-based
90 features, the ImageStreamX Mk II combines the per cell information content provided by

91 standard microscopy with the statistical significance afforded by large sample sizes common to
92 standard flow cytometry.

93 This allowed us to exclude most of the bacterial doublets or small aggregates, and calculate
94 more accurately both the % of positive GFP cells, as well as bacterial cell length and GFP
95 intensity normalized for cell size. This detailed analysis of antibiotic reporters demonstrated that
96 in addition to the % of positive GFP cells for surfactin promoter, the distribution of GFP intensity
97 in the population also changes (Figure 2). These effects were also observed for the transcription
98 from the *bac,* (Figure 3), *pps (*Figure 4) and *pks* promoter (Figure 5). The impact of the plant on
99 cell length was not robust, as it was not detected in all image-stream experiments (Figures 2-
100 5). However, there were experimental sets where the plant significantly affected cell shape and
101 reduced the length of *B. subtilis* cells (Figures 4 and 5).

102 To confirm that the impact of the plant root on antibiotic production could be due to a secreted
103 we monitored the expression from P_{srfAA} and P_{pksC} fused to a luciferase reporter in the presence
104 and absence of root secretions. The use of the unstable luciferase (an enzyme which degrades
105 rapidly and therefore not accumulated (McLoon et al., 2011a) as a reporter allows us to monitor
106 gene expression in real time by monitoring light production in a plate reader with an
107 illuminometer. When grown on liquid defined medium, wild-type cells expressed luciferase from
108 *srfAA* and *pksC* promoters robustly. However, while root secretions did not alter the kinetic of
109 the expression, they were sufficient to significantly increase the intensity of the luciferase
110 emission (Figure 6). These results suggest that the plant may secret metabolite that regulate
111 the production of sufractin and bacillaene. Consistently, using confocal scanning laser
112 microscopy, we could clearly confirm the expression of the *pks* promoter and on some extent,
113 surfactin on cells attached with *A. thaliana* roots (Figure 7).

114 β-lactamases are enzymes which account for an additional layer of defence as they hydrolyse
115 the β-lactam ring of β-lactams, thus inactivating the antibiotic before it reaches its target, the
116 PBPs (Therrien and Levesque, 2000). Consistent with a hypothesis that the plant and tis
117 secretions specifically regulate antibiotic production, the expression of the unrelated PenP
118 promoter was not induced but rather slightly decreased in the presence of the plant (Figure 8).

119

120 **Discussion**

121 Since *B. subtilis* was first described by Ferdinand Cohn in the late 1800s, it was shown to
122 specialize in the production of metabolites (McLoon et al., 2011b). Many of the biosynthetic
123 pathways for these metabolites are conserved either across the entire Bacillus genus or within
124 specific phylogenetic clades. Fengycin, bacillaene, bacilysin and surfactin were essentially
125 observed within the *B. subtilis* group (Hou and Kolodkin-Gal, 2020). This suggests that the
126 different environmental niches inhabited by members of the *B. subtilis* clade may select for
127 conservation of metabolites with distinct (or potentially redundant) beneficial functions.

128 Here, we found that the production of non-ribosomal peptides and polyketides was specifically
129 activated during symbiotic interaction with *A. thaliana*. Our results demonstrated that both the
130 root and its secretions increased the expression of four different biosynthetic clusters encoding
131 for antibiotics with significance for *B. subtilis* competitiveness. In contrast, the PenP β-
132 lactamase which deactivate β-lactam antibiotic was not induced by the host. This result is
133 intriguing as the production of this enzyme promotes increased resistance of the bacterium in
134 the competitive soil environment, containing β-lactam producers (Hou and Kolodkin-Gal, 2020),
135 but does not contribute directly to the fitness of the plant. In contrast, each of the induced
136 antibiotics were shown to grant protection to the plant versus fungal and bacterial pathogens.

137 Interestingly, we previously demonstrated that the interaction with the plant increases the
138 capacity of *B. subtilis* to compete with *Serattia Plymuthica*, and our current results further
139 indicate that the root is active regulator of the competitive interactions occurring on its roots
140 (Ogran et al., 2019). The complexity of these antibiotic-host interactions suggests that *B. subtilis*
141 biofilms can be considered a part of the plant microbiome, with the host actively promoting the
142 establishment of the most beneficial bacterial community. Our findings provide a simple
143 example of high-order interactions that shape microbiomes; the host modulates antibiotic
144 production in the desired bacterial colonizers, providing the colonizers a clear advantage over
145 less beneficial potential residents.

146

147 **Materials and Methods**

148 Strains and media

149 All strains used in this study are in Table S1. The strains were grown in LB broth (Difco), or
150 MSgg medium(Branda et al., 2001) (5 mM potassium phosphate, 100 mM MOPS (pH 7), 2 mM
151 MgCl2, 50 μM MnCl2, 50 μM FeCl3, 700 μM CaCl2, 1 μM ZnCl2, 2 μM thiamine, 0.5% glycerol,

152 0.5% glutamate, 50 µg/mL threonine, tryptophan and phenylalanine) (Branda et al., 2001). Solid
153 LB medium contained 1.5% bacto agar (Difco).

154

155 Plant Growth Conditions

156 Seeds of *A. thaliana* Col-0 were surface-sterilized and seeded on petri dishes containing
157 Murashige and Skoog medium (4.4 g/L), PH 5.7, supplied with 0.5% (w/v) plant agar (Duchefa),
158 0.5% Sucrose (SigmaAldrich) and then stratified at 4°C for 2 days. The seeds were further
159 transferred to a growth chamber (MRC) at 23°C in 12 h light/12 h dark regime.

160

161 Extraction of plant secretions

162 Plant secretions were retrieved from 14-day-old *A. thaliana* seedlings cultured in 6 ml liquid
163 MSgg of each well of a 6-well microplate (Thermo Scientific). 8 seedlings were put in each well.
164 The plant secretions were collected after four days and filtered with a 0.22 µm filter, and stored
165 at 4°C for further use

166

167 Luminescence experiments

168 Luminescence reporters were grown in either MSgg medium or MSgg medium containing plant
169 secretions. Experiments were carried using a 96 – well plate flat bottom with white opaque walls
170 (Corning). Measurements were performed every 30 min at 30 °C for a period for 24h, using a
171 microplate reader (Synergy 2; BioTek, Winooski, VT, USA). Luciferase activity was normalized
172 to avoid artefacts related to differential cells numbers as RLU/OD.

173

174 Confocal microscopy

175 Plants cultured with bacteria were washed in PBS and mounted on a microscope slide and
176 covered with a poly-L-Lysine 31 (Sigma)-treated coverslip. Cells were visualized and
177 photographed using a laser scanning confocal microscope (Zeiss LSM 780) equipped with a
178 high resolution microscopy Axiocam camera, as required. Data were captured using Zen black
179 software (Zeiss, Oberkochenm, Germany).

180

181 Flow Cytometer Cell Sorting

182 Indicated strains used in the experiments were inoculated at an OD of 0.02 in 1.5 ml liquid
183 MSgg without seedlings (control) and MSgg with 14-d-old *A. thaliana* seedlings in a 24-well
184 plate (Thermo Scientific), each well contained four seedling. the set was incubated for 24h in
185 growth chamber (MRC) at 23°C in 12 h light/12 h dark regime. After incubation the seedlings
186 were removed from the liquid medium, washed in PBS and transferred to a 1.5 eppendorf tube
187 in 1 ml of PBS and vortexed for 1 minute, for the purpose of detaching the bacteria from the
188 root. Samples was measured using a BD LSR II flow cytometer (BD Biosciences), using laser
189 excitation of 488 nm, coupled with 505 LP and 525/50 sequential filters.. 100,000 cells were
190 counted and samples were analyzed usingFACS Diva (BD Biosciences).

191

192 Imaging Flow Cytometry

193 Samples were prepared as for the sorting flow cytometer. Data was acquired by ImageStream
194 X mark II (Luminx corp., Austin Tx) using a 60X lense (NA=0.9). Lasers used were 488nm
195 (200mW) for GFP excitation and 785nm (5mW) for side scatter measurement. During
196 acquisition bacterial cells were gated according to their area (in square microns) and side
197 scatter, which excluded the calilbration beads (that run in the instrument along with the sample).
198 For each sample 100,000 events were collected. Data was analysed using IDEAS 6.3. Single
199 event bacteria were selected according to their area (in square microns) and aspect ratio (width
200 divided by the length of a best-fit ellipse).

201

202 Flow Cytometry

203 Indicated strains used in the experiments were inoculated at an OD of 0.02 in 1.5 ml liquid
204 MSgg without seedlings (control) and MSgg with 14-d-old *A. thaliana* seedlings in a 24-well
205 plate (Thermo Scientific), each well contained four seedling. The set was incubated for 24h in
206 growth chamber (MRC) at 23°C in 12 h light/12 h dark regime. After incubation the seedlings
207 were removed from the liquid medium, washed in PBS and transferred to a 1.5 Eppendorf tube
208 in 1 ml of PBS and vortexed for 1 minute, for the purpose of detaching the bacteria from the
209 root. Samples was measured using a BD LSR II flow cytometer (BD Biosciences), using laser
210 excitation of 488 nm, coupled with 505 LP and 525/50 sequential filters. For each sample

211 100,000 cells were counted and samples were analyzed using Diva 8 software (BD
212 Biosciences).

213

214 Imaging Flow Cytometry

215 Samples were prepared as for the sorting flow cytometer. Data was acquired by ImageStream
216 X mark II (AMNIS, part of Luminex corp., Austin Tx) using a 60X lense (NA=0.9). Lasers used
217 were 488nm (200mW) for GFP excitation and 785nm (5mW) for side scatter measurement.
218 During acquisition bacterial cells were gated according to their area (in square microns) and
219 side scatter, which excluded the calibration beads (that run in the instrument along with the
220 sample). For each sample 100,000 events were collected. Data was analysed using IDEAS
221 6.3. Single event bacteria were selected according to their area (in square microns) and aspect
222 ratio (width divided by the length of a best-fit ellipse). Focused events were selected by the
223 Gradient RMS and Contrast features (measures the sharpness quality of an image by detecting
224 large changes of pixel values in the image). Cells expressing GFP were selected using the
225 Intensity (the sum of the background subtracted pixel values within the image) and Max Pixel
226 values (the largest value of the background-subtracted pixels) of the GFP channel (Ch02).GFP
227 expression was quantified using the Mean Pixel feature (the mean of the background-
228 subtracted pixels contained in the input mask). The size of bacteria was quantified using the
229 Length feature (measures the longest part of an object, in microns) of the bright-field image.

230

231 Statistical analysis

232 All experiments were performed three separate and independent times in triplicates, unless
233 stated otherwise. Statistical analyses were performed with GraphPad Prism 9.0 (GraphPad
234 Software, Inc., San Diego, CA).

235

236 **Acknowledgments:** The Kolodkin–Gal laboratory is supported by the Israel Science
237 Foundation grant number 119/16 and ISF-JSPS 184/20 and Israel Ministry of Science - Tashtiot
238 (Infrastructures) - 123402 in Life Sciences and Biomedical Sciences. IKG is supported by an
239 internal grant from the Estate of Albert Engleman provided by the Angel–Faivovich Fund for
240 Ecological Research, and by a research grant from the Benoziyo Endowment Fund for the

Advancement of Science. IKG is a recipient of the Rowland and Sylvia Career Development Chair.

266 **Table S1**

Strain	Description	Source or reference
B. subtilis	Wild type	(Branda et al., 2001)
P_{pksC}-*lux*	*B. subtilis* sacA::P_{pksC}-*lux* (Cm ^{r}), promoter of bacillaene operon tagged to the luciferase reporter integrated in the neutral *SacA* locus	(Ogran et al., 2019)
P_{srfAA}-*lux*	*B. subtilis* sacA::P_{srfAA}-*lux* (Cm ^{r}), promoter of surfactin operon tagged to the luciferase reporter integrated in the neutral *sacA* locus	(Maan et al., 2021)
P_{srfAA}-*yfp*	*B. subtilis sacA*:: P_{srfAA}-*yfp* (Sp ^{r}), promoter of surfactin operon tagged to the YFP reporter integrated in the neutral *amyE* locus	Avigdor Eldar Lab, TAU, Israel
P_{pksC}-*gfp*	*B. subtilis amyE*:: P_{srfAA}-*yfp* (Cm ^{r}), promoter of bacillaene operon tagged to the GFP reporter integrated in the neutral *amyE* locus	(Ogran et al., 2019)
P_{bacA}-*gfp*	*B. subtilis amyE*:: P_{bacA}-*gfp* (Cm ^{r}), promoter of bacilysin operon tagged to the GFP reporter integrated in the neutral *amyE* locus	(Maan et al., 2021)
P_{ppsA}-*gfp*	*B. subtilis amyE*:: P_{ppsA}-*gfp* (Cm ^{r}), promoter of plipstatin operon tagged to the GFP reporter integrated in the neutral *amyE* locus	(Maan et al., 2021)
P_{penP}-*gfp*	*B. subtilis amyE*:: P_{penP}-*gfp* (Sp ^{r}), promoter of plipstatin operon tagged to the GFP reporter integrated in the neutral *amyE* locus	(Bucher et al., 2019)

267

268 **Cm ^{r}** – chloramphenicol resistance, **Sp ^{r}** – spectinomycin resistance

269

270

271

References:

Adam, E., Groenenboom, A.E., Kurm, V., Rajewska, M., Schmidt, R., Tyc, O. et al. (2016) Controlling the Microbiome: Microhabitat Adjustments for Successful Biocontrol Strategies in Soil and Human Gut. *Front Microbiol* **7**: 1079.

Allaband, C., McDonald, D., Vazquez-Baeza, Y., Minich, J.J., Tripathi, A., Brenner, D.A. et al. (2019) Microbiome 101: Studying, Analyzing, and Interpreting Gut Microbiome Data for Clinicians. *Clin Gastroenterol Hepatol* **17**: 218-230.

Arnaouteli, S., Bamford, N.C., Stanley-Wall, N.R., and Kovacs, A.T. (2021) Bacillus subtilis biofilm formation and social interactions. *Nat Rev Microbiol*.

Berg, G., and Raaijmakers, J.M. (2018) Saving seed microbiomes. *ISME J* **12**: 1167-1170.

Berg, G., Koberl, M., Rybakova, D., Muller, H., Grosch, R., and Smalla, K. (2017) Plant microbial diversity is suggested as the key to future biocontrol and health trends. *FEMS Microbiol Ecol* **93**.

Branda, S.S., Gonzalez-Pastor, J.E., Ben-Yehuda, S., Losick, R., and Kolter, R. (2001) Fruiting body formation by Bacillus subtilis. *Proc Natl Acad Sci U S A* **98**: 11621-11626.

Bucher, T., Keren-Paz, A., Hausser, J., Olender, T., Cytryn, E., and Kolodkin-Gal, I. (2019) An active beta-lactamase is a part of an orchestrated cell wall stress resistance network of Bacillus subtilis and related rhizosphere species. *Environ Microbiol*.

Butcher, R.A., Schroeder, F.C., Fischbach, M.A., Straight, P.D., Kolter, R., Walsh, C.T., and Clardy, J. (2007) The identification of bacillaene, the product of the PksX megacomplex in Bacillus subtilis. *Proc Natl Acad Sci U S A* **104**: 1506-1509.

Falardeau, J., Wise, C., Novitsky, L., and Avis, T.J. (2013) Ecological and mechanistic insights into the direct and indirect antimicrobial properties of Bacillus subtilis lipopeptides on plant pathogens. *Journal of chemical ecology* **39**: 869-878.

Fan, B., Blom, J., Klenk, H.P., and Borriss, R. (2017) Bacillus amyloliquefaciens, Bacillus velezensis, and Bacillus siamensis Form an" Operational Group B. amyloliquefaciens" within the B-subtilis Species Complex. *Frontiers in Microbiology* **8**.

Gonzalez, D.J., Haste, N.M., Hollands, A., Fleming, T.C., Hamby, M., Pogliano, K. et al. (2011) Microbial competition between Bacillus subtilis and Staphylococcus aureus monitored by imaging mass spectrometry. *Microbiology* **157**: 2485-2492.

Hou, Q., and Kolodkin-Gal, I. (2020) Harvesting the complex pathways of antibiotic production and resistance of soil bacilli for optimizing plant microbiome. *FEMS Microbiol Ecol*.

Inaoka, T., Takahashi, K., Ohnishi-Kameyama, M., Yoshida, M., and Ochi, K. (2003) Guanine nucleotides guanosine 5'-diphosphate 3'-diphosphate and GTP co-operatively regulate the production of an antibiotic bacilysin in Bacillus subtilis. *J Biol Chem* **278**: 2169-2176.

Kinsella, K., Schulthess, C.P., Morris, T.F., and Stuart, J.D. (2009) Rapid quantification of Bacillus subtilis antibiotics in the rhizosphere. *Soil Biology and Biochemistry* **41**: 374-379.

Kloepper, J.W., Ryu, C.M., and Zhang, S. (2004a) Induced Systemic Resistance and Promotion of Plant Growth by Bacillus spp. *Phytopathology* **94**: 1259-1266.

Kloepper, J.W., Ryu, C.M., and Zhang, S. (2004b) Induced Systemic Resistance and Promotion of Plant Growth by Bacillus spp. *Phytopathology* **94**: 1259-1266.

Kluge, B., Vater, J., Salnikow, J., and Eckart, K. (1988) Studies on the Biosynthesis of Surfactin, a Lipopeptide Antibiotic from Bacillus-Subtilis Atcc-21332. *Febs Letters* **231**: 107-110.

Maan, H., Friedman, J., and Kolodkin-Gal, I. (2021) Resolving the conflict between antibiotic production and rapid growth by recognition of peptidoglycan of susceptible competitors. *bioRxiv*: 2021.2002.2007.430110.

Magnuson, R., Solomon, J., and Grossman, A.D. (1994) Biochemical and genetic characterization of a competence pheromone from B. subtilis. *Cell* **77**: 207-216.

319 McLoon, A.L., Kolodkin-Gal, I., Rubinstein, S.M., Kolter, R., and Losick, R. (2011a) Spatial
320 regulation of histidine kinases governing biofilm formation in Bacillus subtilis. *J Bacteriol* **193**: 679-
321 685.
322 McLoon, A.L., Guttenplan, S.B., Kearns, D.B., Kolter, R., and Losick, R. (2011b) Tracing the
323 domestication of a biofilm-forming bacterium. *J Bacteriol* **193**: 2027-2034.
324 Nagorska, K., Bikowski, M., and Obuchowski, M. (2007) Multicellular behaviour and production of a
325 wide variety of toxic substances support usage of Bacillus subtilis as a powerful biocontrol agent. *Acta*
326 *Biochim Pol* **54**: 495-508.
327 Ogran, A., Yardeni, E.H., Keren-Paz, A., Bucher, T., Jain, R., Gilhar, O., and Kolodkin-Gal, I. (2019)
328 The plant host induces antibiotic production to select the most beneficial colonizers. *Appl Environ*
329 *Microbiol*.
330 Ongena, M., and Jacques, P. (2008) Bacillus lipopeptides: versatile weapons for plant disease
331 biocontrol. *Trends Microbiol* **16**: 115-125.
332 Stein, T. (2005) Bacillus subtilis antibiotics: structures, syntheses and specific functions. *Molecular*
333 *Microbiology* **56**: 845–857
334 Straight, P.D., Fischbach, M.A., Walsh, C.T., Rudner, D.Z., and Kolter, R. (2007) A singular
335 enzymatic megacomplex from Bacillus subtilis. *Proc Natl Acad Sci U S A* **104**: 305-310.
336 Therrien, C., and Levesque, R.C. (2000) Molecular basis of antibiotic resistance and beta-lactamase
337 inhibition by mechanism-based inactivators: perspectives and future directions. *FEMS Microbiol Rev*
338 **24**: 251-262.
339 Tsuge, K., Matsui, K., and Itaya, M. (2007) Production of the non-ribosomal peptide plipastatin in
340 Bacillus subtilis regulated by three relevant gene blocks assembled in a single movable DNA segment.
341 *J Biotechnol* **129**: 592-603.
342

343

344

345

346

347

348

349

350

351

352

353

354

355 **Figure Legends:**

356 Figure 1:

357 Indicated reporter strains for P_{srfAA}-gfp (surfactin), P_{pksC}-gfp (bacillaene), P_{bacA}-gfp (bacilysin)
358 and P_{ppsA}-gfp (plipastatin), were analysed by flow cytometry for (A) positively expressing
359 fluorescent populations or (B) the mean intensity of the fluorescent populations. Reporter stains
360 were either grown in MSgg medium or in MSgg medium in presence of *A. thaliana* seedlings.
361 Data were collected from 24 h post inoculation, 100,000 cells were counted. Graphs represent
362 results from three independent experiments with n = 3/experiment (total n = 9/group). Statistical
363 analysis was performed using Two-way ANOVA followed by Tukey's multiple comparison post
364 hoc testing. $P < 0.05$ was considered statistically significant.

365

366 Figure 2:

367 The expression of P_{srfAA}-gfp (surfactin) attached to plant roots versus cultured in liquid MSgg.
368 Bacteria expressing GFP under the control of the *srf* promoter were cultured in the absence or
369 presence of *A. thaliana* seedlings. After 24h, bacteria colonizing the roots and bacteria cultured
370 in liquid MSgg alone were collected. The percent of GFP expressing cells (**A**), cell length (**B**)
371 and mean fluorescence intensity of the cells (**C**) were measured by Imaging Flow Cytometry
372 and analyzed with IDEAS 6.3. (**D**) Representative bright field and fluorescent images related to
373 expression of GFP in MSgg and on *A. thaliana* roots. Scale bar = 7 µm. Data were collected
374 from 24 h post inoculation, 100,000 cells were counted. Graphs represent results from three
375 independent experiments with n = 3/experiment (total n = 9/group). Statistical analysis was
376 performed using unpaired t-test with Welch correction. $P < 0.05$ was considered statistically
377 significant.

378

379 Figure 3:

380 The expression of P_{pksC}-gfp (bacillaene) attached to plant roots versus cultured in liquid MSgg.
381 Bacteria expressing GFP under the control of the *pks* promoter were cultured in the absence
382 or presence of *A. thaliana* seedlings. After 24h, bacteria colonizing the roots and bacteria
383 cultured in liquid MSgg alone were collected. The percent of GFP expressing cells (**A**), cell
384 length (**B**) and mean fluorescence intensity of the cells (**C**) were measured by Imaging Flow

385 Cytometry and analyzed with IDEAS 6.3. (**D**) Representative brightfield and fluorescent images
386 related to expression of GFP in MSgg and on *A. thaliana* roots. Scale bar = 7 µm. Data were
387 collected from 24 h post inoculation, 100,000 cells were counted. Graphs represent results from
388 three independent experiments with n = 3/experiment (total n = 9/group). Statistical analysis
389 was performed using unpaired t-test with Welch correction. $P < 0.05$ was considered
390 statistically significant.

391

392 Figure 4:

393 The expression of P_{bacA}-gfp (bacilysin) attached to plant roots versus cultured in liquid MSgg.
394 Bacteria expressing GFP under the control of the *bac* promoter were cultured in the absence
395 or presence of *A. thaliana* seedlings. After 24h, bacteria colonizing the roots and bacteria
396 cultured in liquid MSgg alone were collected. The percent of GFP expressing cells (**A**), cell
397 length (**B**) and mean fluorescence intensity of the cells (**C**) were measured by Imaging Flow
398 Cytometry and analyzed with IDEAS 6.3 (**D**) Representative brightfield and fluorescent images
399 related to expression of GFP in MSgg and on *A. thaliana* roots. Scale bar = 7 µm. Data were
400 collected from 24 h post inoculation, 100,000 cells were counted. Graphs represent results from
401 three independent experiments with n = 3/experiment (total n = 9/group). Statistical analysis
402 was performed using unpaired t-test with Welch correction. $P < 0.05$ was considered
403 statistically significant.

404

405 Figure 5:

406 The expression of P_{ppsA}-gfp (plipastatin) in bacteria attached to plant roots versus cultured in
407 liquid MSgg. Bacteria expressing GFP under the control of the *pps* promoter were cultured in
408 the absence or presence of *A. thaliana* seedlings. After 24h, bacteria colonizing the roots and
409 bacteria cultured in liquid MSgg alone were collected. The percent of GFP expressing cells (**A**),
410 cell length (**B**) and mean fluorescence intensity of the cells (**C**) were measured by Imaging Flow
411 Cytometry and analyzed with IDEAS 6.3. (**D**) Representative brightfield and fluorescent images
412 related to expression of GFP in MSgg and on *A. thaliana* roots. Scale bar = 7 µm. Data were
413 collected from 24 h post inoculation, 100,000 cells were counted. Graphs represent results from
414 three independent experiments with n = 3/experiment (total n = 9/group). Statistical analysis

415 was performed using unpaired t-test with Welch correction. $P < 0.05$ was considered
416 statistically significant.

417

418 Figure 6:

419 *A. thaliana* secretions increase the expression of (A) P_{srfAA}-lux (surfactin) and (B) P_{pksC}-
420 lux (bacilllane) in *B. subtilis* cells. Bacteria expressing luciferase under the control of the *srf* and
421 *pks* promoters were cultured in *A. thaliana* secretions or in liquid MSgg and grown in a
422 microplate reader for 24h. Graphs represent results from three independent experiments. Error
423 bars represent ± SEM.

424

425 Figure 7:

426 The expression of P_{pksC}-gfp (bacillaene) and P_{srfAA}-gfp (surfactin) on *A. thaliana* roots. Bacteria
427 expressing GFP under the control of the *pks* and *srf* promoters were cultured in the presence
428 of *A. thaliana* seedlings in MSgg medium. After 24h, the bacteria colonizing the roots were
429 photographed with confocal microscope.

430

431 Figure 8:

432 Indicated reporter strains for P_{penP}-gfp was analysed by flow cytometry for (A) positively
433 expressing fluorescent populations or (B) the mean intensity of the fluorescent populations.
434 Reporter stains were either grown in MSgg medium or in MSgg medium in presence of *A.*
435 *thaliana* seedlings.

436

437

Figure 1

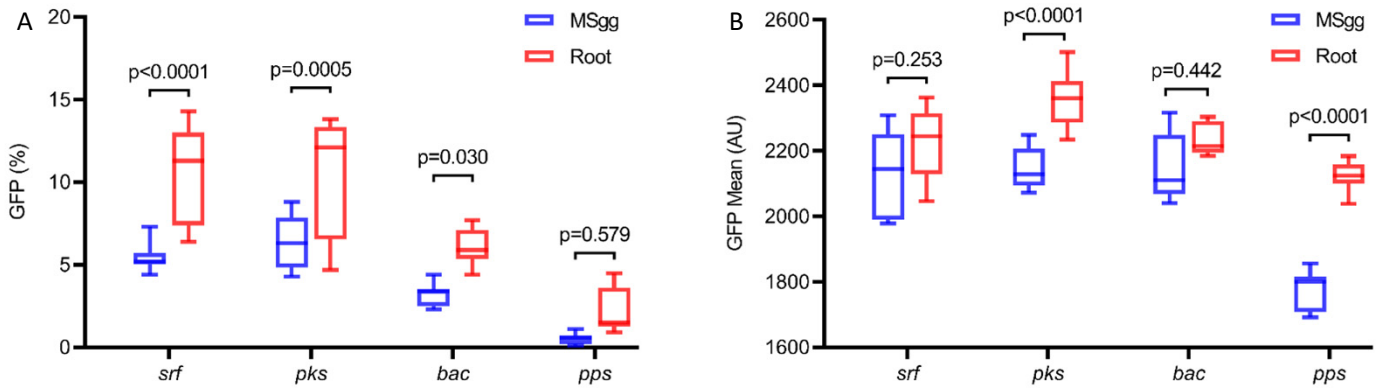
A
GFP (%)
20
15
10
5
0
MSgg
Root
p<0.0001
p=0.0005
p=0.030
p=0.579
srf
pks
bac
pps
B
GFP Mean (AU)
2600
2400
2200
2000
1800
1600
MSgg
Root
p=0.253
p<0.0001
p=0.442
p<0.0001
srf
pks
bac
pps

Figure 2

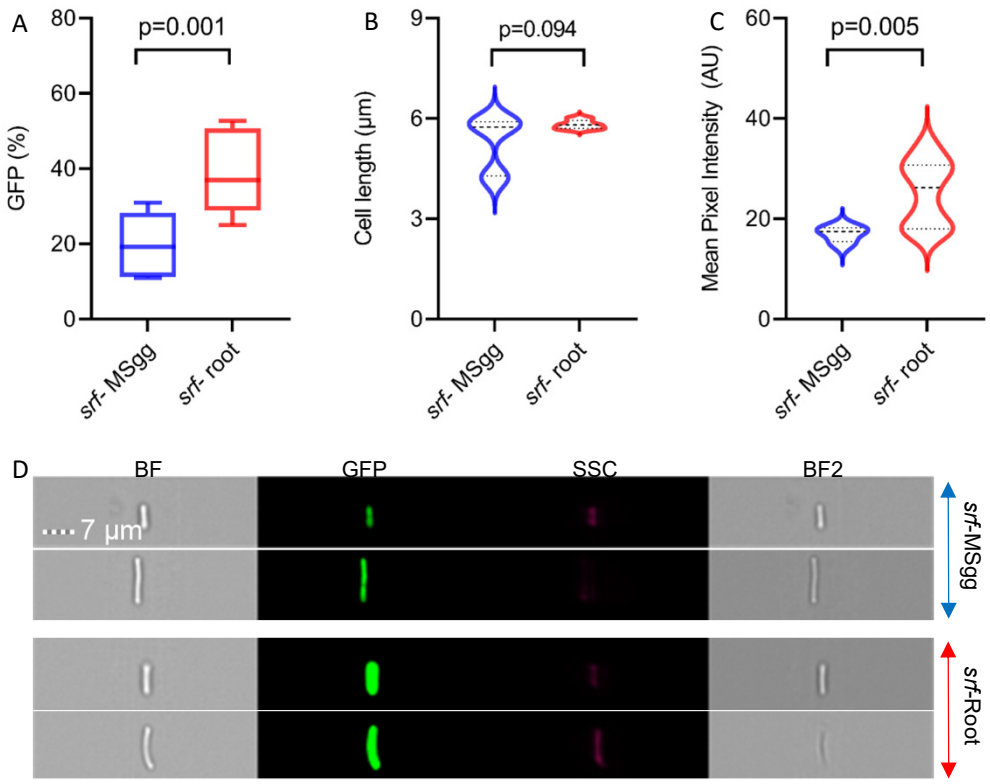
A
p=0.001
GFP (%)
80
60
40
20
0
srf- MSgg
srf- root
B
p=0.094
Cell length (µm)
9
6
3
0
srf- MSgg
srf- root
C
p=0.005
Mean Pixel Intensity (AU)
60
40
20
0
srf- MSgg
srf- root
D
BF
GFP
SSC
BF2
7 µm
srf-MSgg
srf-Root

Figure 3

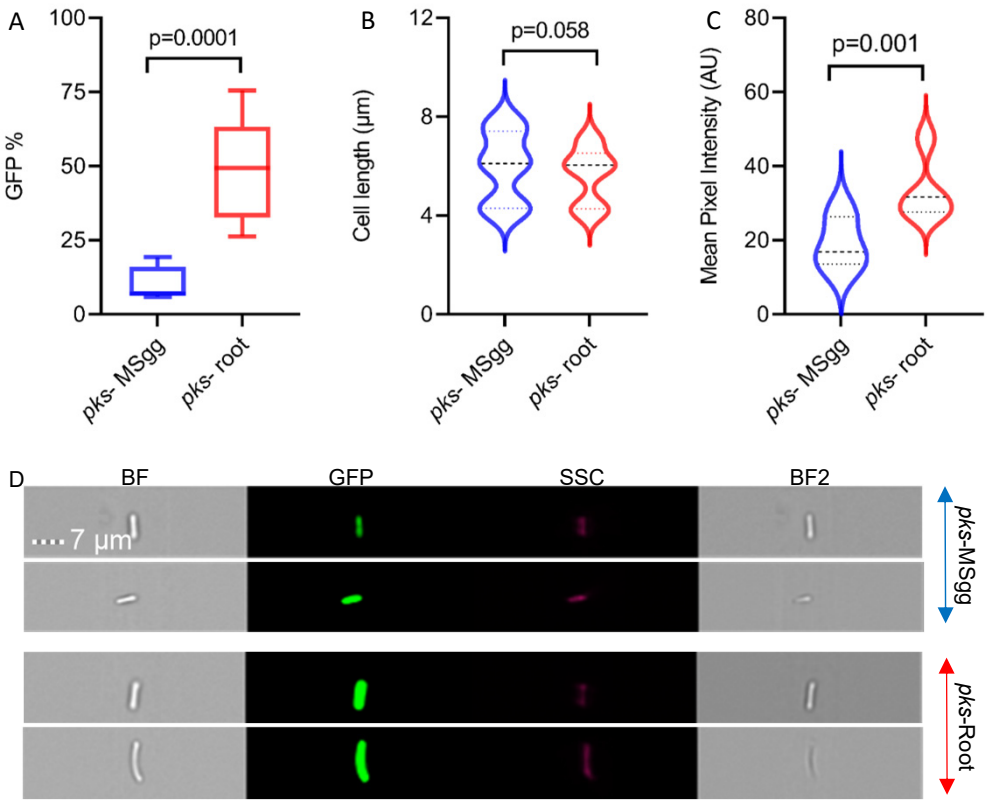
A
GFP %
100
75
50
25
0
p=0.0001
pks- MSgg
pks- root
B
Cell length (µm)
12
8
4
0
p=0.058
pks- MSgg
pks- root
C
Mean Pixel Intensity (AU)
80
60
40
20
0
p=0.001
pks- MSgg
pks- root
D
BF
GFP
SSC
BF2
7 µm
pks-MSgg
pks-Root

Figure 4

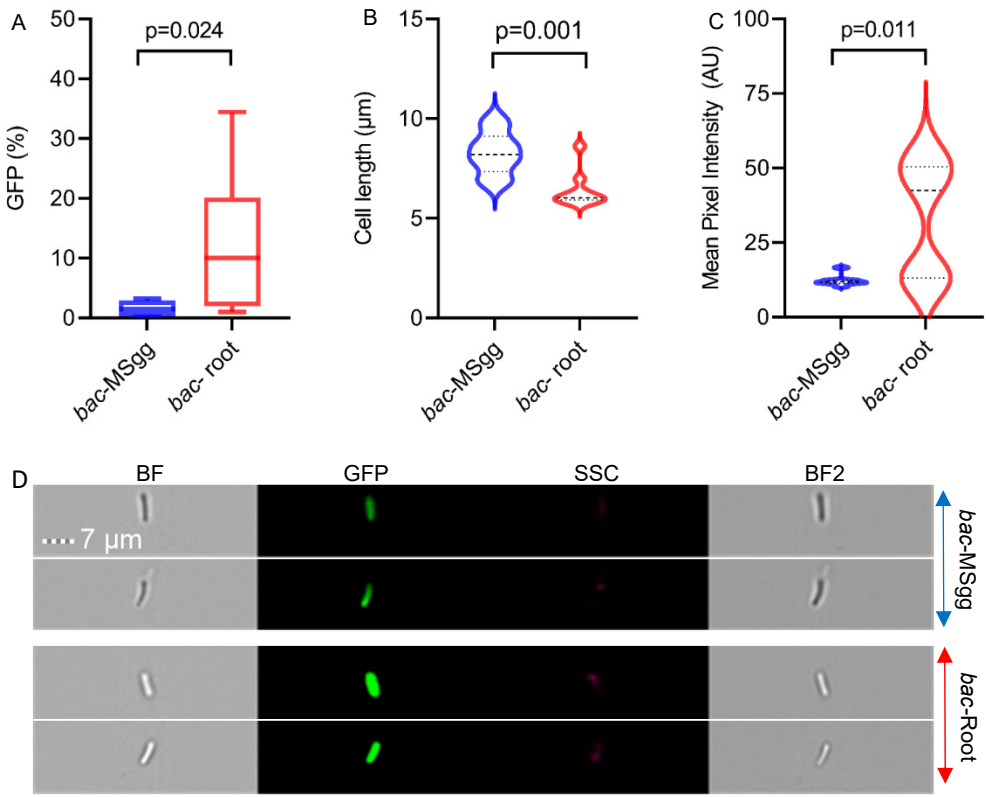
A
p=0.024
GFP (%)
50
40
30
20
10
0
bac-MSgg
bac- root
B
p=0.001
Cell length (µm)
15
10
5
0
bac-MSgg
bac- root
C
p=0.011
Mean Pixel Intensity (AU)
100
75
50
25
0
bac-MSgg
bac- root
D
BF
GFP
SSC
BF2
7 µm
bac-MSgg
bac-Root

Figure 5

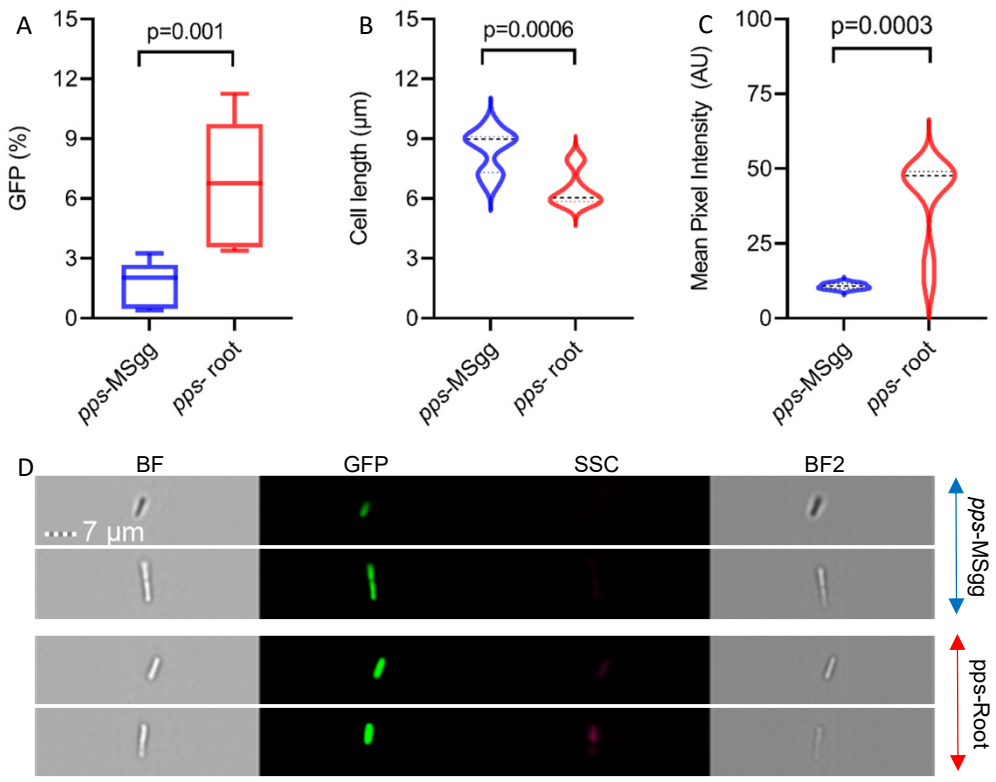
A
p=0.001
GFP (%)
15
12
9
6
3
0
pps-MSgg
pps- root
B
p=0.0006
Cell length (µm)
15
12
9
6
3
0
pps-MSgg
pps- root
C
p=0.0003
Mean Pixel Intensity (AU)
100
75
50
25
0
pps-MSgg
pps- root
D
BF
GFP
SSC
BF2
7 µm
pps-MSgg
pps-Root

Figure 6

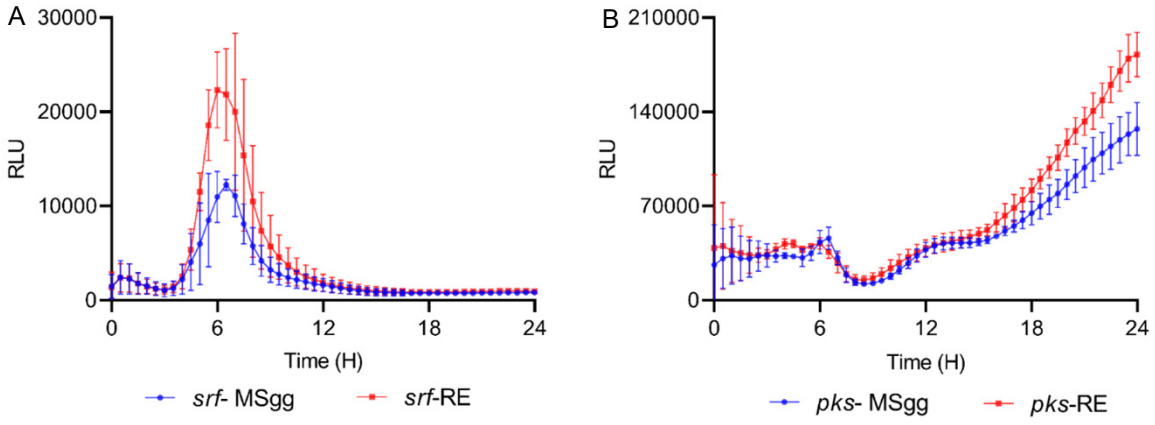
A
30000
20000
10000
0
RLU
0
6
12
18
24
Time (H)
srf- MSgg
srf-RE
B
210000
140000
70000
0
RLU
0
6
12
18
24
Time (H)
pks- MSgg
pks-RE

Figure 7

WT

P_{pks}-*gfp*

P_{srfAA}-*gfp*

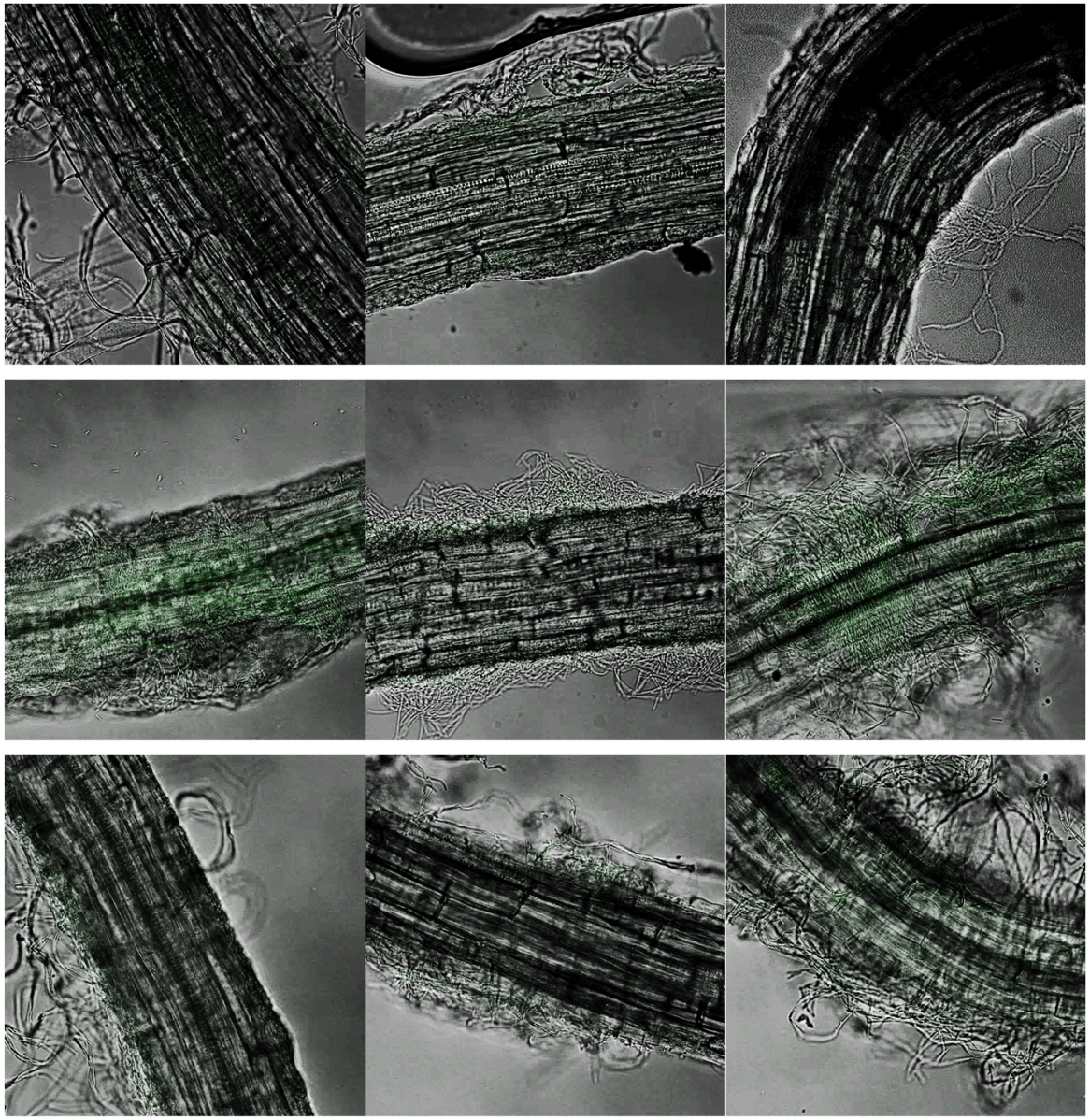

Figure 8

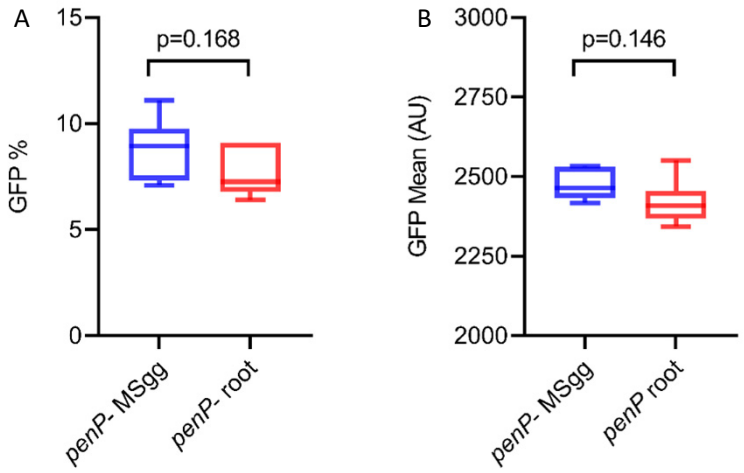
A
15
10
5
0
GFP %
p=0.168
penP- MSgg
penP- root
B
3000
2750
2500
2250
2000
GFP Mean (AU)
p=0.146
penP- MSgg
penP root